Acta Scientiarum

http://www.uem.br/acta
ISSN printed: 1806-2563
ISSN on-line: 1807-8664
Doi: 10.4025/actascitechnol.v28i2.27440

Photodegradation of sugarcane vinasse: evaluation of the effect of vinasse pre-treatment and the crystalline phase of TiO_2

Renata Padilha de Souza[1*], Ana Maria Ferrari-Lima[2], Osvaldo Pezoti[3], Veronice Sluzarski Santana[4], Marcelino Luiz Gimenes[5] and Nádia Regina Camargo Fernandes-Machado[5]

*[1]Coordenação de Bioprocessos e Biotecnologia, Universidade Tecnológica Federal do Paraná, Estrada para Boa Esperança, Km 04, 85660-000, Dois Vizinhos, Paraná, Brazil. [2]Coordenação de Tecnologia em Processos Químicos, Universidade Tecnológica Federal do Paraná, Apucarana, Paraná, Brazil. [3]Departamento de Química, Universidade Estadual de Maringá, Maringá, Paraná, Brazil. [4]Departamento de Engenharia Química, Universidade Estadual do Oeste do Paraná, Toledo, Paraná, Brazil. [5]Departamento de Engenharia Química, Universidade Estadual de Maringá, Maringá, Paraná, Brazil. *Author for correspondence. E-mail: rpspadilha@hotmail.com*

ABSTRACT. In this work, the effect of vinasse pre-treatment and anatase content in the photocatalytic degradation of sugarcane vinasse was evaluated. The *in nature* vinasse was pretreated by coagulation/flocculation using vegetal tannin as coagulant and diluted 1: 2 with deionized water. The photocatalytic tests with *in nature*, pretreated and diluted vinasse were performed for 48 hours under UV radiation using 1 g of catalyst: TiO_2 Kronos calcined at 300ºC (100% anatase) and 1000ºC (34% anatase) and TiO_2 P25 (87% anatase). The process of coagulation/flocculation removed about 50, 85 and 97% of COD, color and turbidity of *in nature* vinasse, respectively. The results showed that despite the slight COD decrease of *in nature* vinasse, its toxicity was significantly reduced after photocatalytic treatment, especially when TiO_2-34 and TiO_2-87 were used. This behavior shows that the mixture of anatase and rutile phases showed a positive synergistic effect. Regarding pre-treatment of vinasse, the coagulation/flocculation process was more efficient, promoting the greatest reductions of COD (67%) and toxicity (up to 10 times).

Keywords: vinasse, coagulation/flocculation, photocatalysis, toxicity.

Fotodegradação da vinhaça: avaliação do efeito do pré-tratamento da vinhaça e da fase cristalina do TiO_2

RESUMO. Neste trabalho, foi avaliado o efeito do pré-tratamento da vinhaça e do teor de anatase na degradação fotocatalítica da vinhaça. A vinhaça *in natura* foi pré-tratada por coagulação/floculação usando tanino vegetal como coagulante e diluição 1:2 com água deionizada. Os testes fotocatalíticos com a vinhaça *in natura*, pré-tratada e diluída foram realizados durante 48h sob radiação UV utilizando 1 g de catalisador: TiO_2 Kronos calcinado a 300ºC (100% anatase) e a 1000ºC (34% anatase) e TiO_2 P25 (87% anatase). O processo de coagulação/floculação removeu cerca de 50, 85 e 97% de DQO, cor e turbidez da vinhaça *in natura*, respectivamente. Os resultados mostraram que apesar da pequena redução de DQO da vinhaça *in natura*, sua toxicidade foi reduzida significativamente após tratamento fotocatalítico, principalmente quando TiO_2-34 e TiO_2-87 foram utilizados. Esse comportamento evidencia que a mistura das fases anatase e rutile apresentou efeito sinérgico positivo. Em relação ao pré-tratamento da vinhaça, o processo de coagulação/floculação se mostrou mais eficiente, promovendo as maiores reduções de DQO (67%) e toxicidade (até 10 vezes).

Palavras-chave: vinhaça, coagulação/floculação, fotocatálise, toxicidade.

Introduction

The demand for sustainable and clean energy sources has led Brazil to invest in the production of ethanol from sugarcane. Ethanol is a renewable energy source, a green fuel that mitigates the effect of greenhouse gases (Furtado, Scandiffio, & Cortez, 2011). In Brazil, pure and gasoline-blended kinds of ethanol are used as automobile fuels. The consumption of both ethanol and sugar has increased worldwide. However, ethanol and sugar production technologies cause a huge problem: the production of vinasse, a pollutant considered one hundred times more harmful than domestic residues (Silva, Griebeler, & Borges, 2007). Vinasse is one of the most recalcitrant industrial effluents. It is estimated that the mid-south region of Brazil produced a total of 2.30 billion L of ethanol (anhydrous and hydrated) in March 2015, together with around 30 billion L of vinasse (União da Indústria de Cana-de-Açúcar [Unica], 2015).

Nowadays Brazilian farmers employ *in nature* vinasse as a fertilizer in the sugarcane culture

because of its valuable mineral content (Silva, Griebeler, & Borges, 2007). However, due to the toxic organic compounds that it contains, such as phenol derivatives and brown-colored polymers (melanoidin), both compound classes that show chemical stability and are hard to decompose in the environmental conditions, this is not an environmentally correct waste management (Mohana, Acharya, & Madamwar, 2009). Additionally, skatol and other sulfur compounds are also undesirable due to their unpleasant smell (Sharma et al., 2007). In fact, some researchers have detected changes in underground water quality, soil pH leading to micronutrient deficiency due to metal complexation, and other adverse effects in fields where vinasse was applied (Rosabal et al., 2007). Acid pH and high chemical oxygen demand (COD) and biochemical oxygen demand (BOD) contribute to the recalcitrant nature of vinasse, which is classified as a persistent organic pollutant.

Traditional wastewater treatment methodologies are unable to eliminate or transform vinasse into less toxic products (Mohana et al., 2009). Therefore, the ethanol-sugar industry has been forced to search new wastewater treatments that ally economic benefits and efficiency (Andreozzi et al., 1999). Among the vinasse treatments, coagulation/flocculation process (Couto Junior, Barros, & Pereira, 2013) and aerobic (Cibis, Ryznar-Luty, Krzywonos, & Miskiewicz, 2007) and anaerobic digestion (Martín, Raposo, Borja, & Martn, 2002) have been studied. However, these treatments are not satisfactory because of low efficiency or difficult application in industrial scale with large vinasse volumes. The development of new vinasse treatment methods became necessary and the heterogeneous photocatalysis, an advanced oxidation process (AOP), is an interesting option (Santana & Fernandes-Machado, 2008; Brites, Santana, & Fernandes-Machado, 2011). Light and TiO_2 catalyst have been used as a redox system capable of mineralizing organic pollutants (Robert & Malato, 2002) in wastewater from several types of industries: textile dyes (Garcia, Simionato, Silva, Nozaki, & Souza, 2009), petrol station wastewater (Ferrari-Lima, Marques, Fernandes-Machado, & Gimenes, 2013) and pesticide (Ahmed, Rasul, Brown, & Hashib, 2011). All studies have reported good results for color, turbidity, COD and toxicity reduction.

TiO_2 catalyst is one of the most studied in photocatalysis due to high photocatalytic activity, low costs, low toxicity and high photochemical stability (Nogueira & Jardim, 1998). It is found in three crystalline phases: brookite (orthorhombic), anatase (tetragonal) and rutile (tetragonal), wherein the anatase and rutile phases are commonly used in photocatalysis, which the anatase phase is considered the highest catalytic activity (Linsebigler, Lu, & Yates, 1995). The photocatalytic activity depends on the structural and surface properties such as specific area, bandgap, porosity, particle size distribution and density of surface hydroxyl (Ahmed et al., 2011).

The performance of the organic material degradation is largely known including several pathways that lead the adsorbed water and hydroxide ions at TiO_2 surface to produce hydroxyl radicals, $HO^{\bullet}$, the most relevant oxidant species formed (Boroski et al., 2008). However, for the successful of photocatalysis, COD values must be lower than 800 mgL^{-1} due to the high suspended material content that leads to light scattering effects, preventing the catalyst activation. In addition, organic matter tends to recover the catalyst surface, which could diminish the amount of photons that reaches photo-reactive sites on TiO_2 (Gogate & Pandit, 2004). An alternative is to combine photocatalysis to previous physical–chemical procedure, a pre-treatment, such as coagulation/flocculation process, where coagulant agents interact with colloidal materials by either charge neutralization or adsorption, leading to coagulation/flocculation followed by sedimentation to eliminate most of the organic matter. Thus, the aim of this study was to evaluate the influence of vinasse pre-treatment (coagulation/flocculation and dilution) and anatase content of TiO_2 in the photocatalytic degradation of vinasse.

Material and methods

TiO_2 catalysts

Samples of TiO_2 with or without thermal treatment to have different crystalline phases were used dispersed in solution: TiO_2 (Kronos) calcined at 300 and 1000°C for 4 hours and TiO_2 P25 (Evonik-Degussa) without thermal treatment. The catalysts were submitted to a particle agglomeration process with particle size between 0.150 - 0.300 mm, to facilitate recovery at the end of reaction.

Catalyst characterization

The crystalline structure of catalysts was analyzed with X-ray XRD diffractometer (Shimadzu model D6000, mode 2θ with a CuKα source, 40 KV, 30 mA, rate 0.2 min^{-1}) using the JCPDS database (Joint Commite on Powder Diffraction Standars [JCPDS], 1995). The textural properties of catalysts were characterized by N_2 adsorption-desorption isotherms at 77 K, using a QuantaChrome Nova

1200 surface area analyzer. The surface area was determined by BET method, total pores volume was calculated in the P P_0^{-1} = 0.99 and micropores volume was calculated using the t-method. Photoacoustic spectroscopy (PAS) was performed using monochromatic light provided by a xenon 1000 W lamp (Oriel Corporation 68820), a monochromator (Oriel Instruments 77250), a high-sensitivity capacitive microphone (Bruel and Kjaer) and a lock-in amplifier (EG & G5110). The photoacoustic spectrum was obtained at a modulation frequency of 21 Hz and wavelength from 200 to 800 nm. The zero point charge (pH_{zpc}) of each catalyst was determined by agitating a suspension (1 g of catalyst and 30 mL of deionized water) for 24 hours and then measuring the pH (Fernandes-Machado & Santana, 2005).

Vinasse

Vinasse from sugarcane ethanol-sugar industry was obtained from a mill located in northwestern Paraná State, Brazil. Samples were collected during the sugarcane crop/processing season, directly from the distillation column, with temperature around 100ºC. The samples were maintained at 5ºC and used within one week's time. The vinasse was characterized in terms of pH, color (PtCo-APHA) at 455 nm, turbidity (FTU) at 860 nm and COD (mgO_2 L^{-1}) at 600 nm using a Hach DR/2010 spectrophotometer in accordance with standard methods (American Public Health Association [Apha], 1999).

Vinasse pre-treatment

Vinasse samples were subjected to simple dilution with deionized water in the ratio 1:2 (v v^{-1}) and coagulation/flocculation process. Coagulation/flocculation was conducted in a Milan JT101 jar test at room temperature with vegetal tannin Tanfloc® SG in liquid state (Tanac S/A) as coagulant. The best experimental clarification parameters were previously determined (Souza, Girardi, Santana, Fernandes-Machado, & Gimenes, 2013). 600 mL of *in nature* vinasse were mixed with 150 mL of vegetal tannin 10% (v v^{-1}) obtained by dilution of commercial Tanfloc® SG. The samples were mixed at 100 rpm for 1 min, followed by slow mixing at 50 rpm for 30 min and finally rested for 24 hours for sedimentation. The mixtures were maintained at natural pH of vinasse (4.7).

Photodegradation experiments

The photodegradation experiments were conducted in a glass batch photoreactor with dimensions 40 x 25 x 7 cm (length x width x depth), as images shown in Figure 1, using artificial UV irradiation provided by germicide lamp (OSRAM 15 W). The photoreactor was placed at 20 cm away from the light source. The emission spectrum of germicide lamp was determined in a VS140 Linear Array UV-Vis & Vis spectrometer (Horiba).

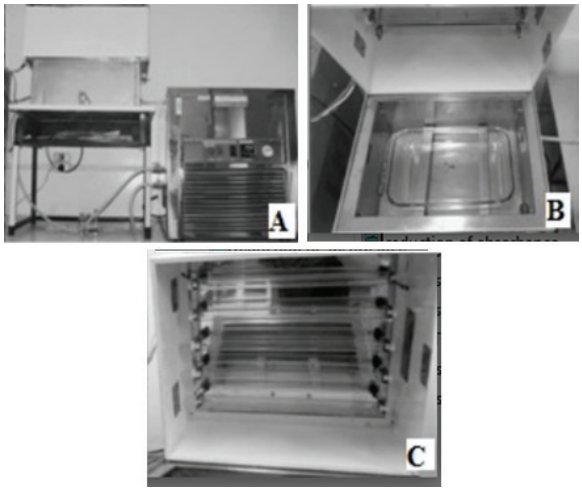

Figure 1. (A) Photoreactor, (B) Internal view of the photoreactor and (C) Germecide lamp position.

The photocatalytic tests were carried out with 1.0 g of catalyst dispersed in 1 L of vinasse (*in nature*, diluted or pre-treated by coagulation/flocculation) at natural pH (4.7) and temperature around 25ºC and they lasted 48 h. Aliquots were collected in the reaction times of 2, 4, 6, 8, 24, 32 and 48 hours and analyzed by UV-Vis spectrophotometry (HACH Lange CADAS-DR 5000) obtaining the percentage of absorbance reduction (Equation 1) at 254 nm (aliphatic region), 284 nm (aromatic groups like phenols), 310 nm (conjugated aromatic rings) and 500 nm (visible light-absorbing molecules).

$$\% \text{ of Reduction} = \frac{Abs_o - Abs}{Abs_o} x100 \quad (1)$$

where:

Abs_o is the initial absorbance and,

Abs is the absorbance after 48 hours of irradiation.

Toxicity bioassays: *Artemia salina*

Microcrustacean brine shrimp (*Artemia salina L.*) was employed as a biological indicator of acute toxicity, acting as a test organism in a variety of toxicological tests. This bioassay was carried out following a protocol presented by Souza, Girardi, Santana, Fernandes-Machado, and Gimenes (2013): Cysts-like eggs of *Artemia salina* were incubated in synthetic seawater (20 g L^{-1} NaCl in water) for about

24 hours at 28ºC with continuous illumination and aeration. After the cysts had hatched, 6-11 nauplii were selected and added in multi-well plates with 1 mL of NaCl solution (20 g L^{-1}) and 0, 0.1, 0.3, 0.7 and 1.0 mL of the sample. Potassium dichromate was used as control experiment (1 mL of NaCl solution (20 g L^{-1}) and 0, 10, 20, 40 and 60 µL of the $K_2Cr_2O_7$). The mortality of microcrustaceans for each sample allowed estimating the lethal concentration for 50% of the nauplii (LC_{50}) through the Reed-Muench plot (Santana & Fernandes-Machado, 2008; Souza et al., 2013).

Results and discussion

Catalyst characterization

The catalysts were characterized by XRD and the diffractograms can be visualized in the Figure 2. The characterization results of the TiO_2 Kronos without thermal treatment were shown for comparison with other catalysts. The XRD diffractograms analyzed with the JCPDS database allowed the identification of TiO_2 anatase and rutile crystalline phases. The relative quantification of these phases was performed according to the Equation 2:

$$X_R = \frac{I_R / I_A * K}{1 + I_R / I_A * K} \quad (2)$$

where:

I_R and I_A are the diffraction peak intensities of the rutile and anatase phases at 2θ values of 27.42 and 25.46, respectively. K is a constant equal to 0.79 (Yang, Li, Wang, Yang, & Lu, 2002).

From analysis of the diffraction patterns (Figure 2) and Equation 2, it was found that the TiO_2 P25 without thermal treatment showed 86.6% of anatase and 13.4% of rutile (labeled TiO_2-87), while TiO_2 Kronos presented 100% anatase phase without thermal treatment. The thermal treatment of TiO_2 Kronos at 300ºC produced no phase change (100% anatase) (labeled TiO_2-100). TiO_2 (Kronos) calcined at 1000ºC exhibited 33.5% anatase and 66.5% rutile phases (labeled TiO_2-34).

The textural properties of the catalysts were evaluated from adsorption-desorption isotherms of N_2 at 77 K and these isotherms are shown in Figure 3. It can be seen that the catalysts had adsorption-desorption isotherm profile very close to type II, with low surface area and low microporosity (TiO_2-87), similar results were found in previous works by Santana and Fernandes-Machado (2008) and Santana, Alberton, and Fernandesmachado (2005).

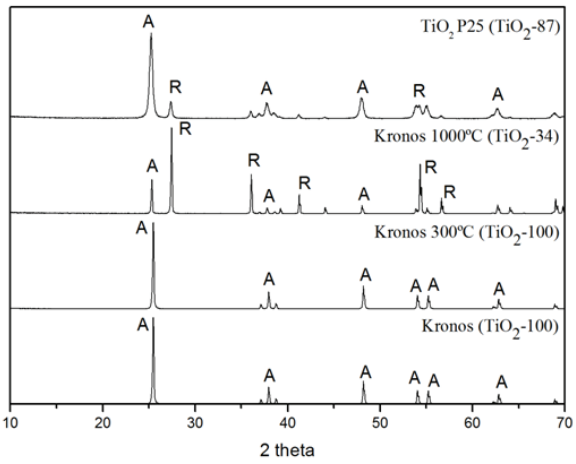

Figure 2. XRD diffractograms of the catalysts: TiO_2 P25 Degussa (TiO_2-87), Kronos calcined at 300ºC (TiO_2-100) and at 1000ºC (TiO_2-34) and Kronos without thermal treatment (TiO_2-100). A: anatase and R: rutile.

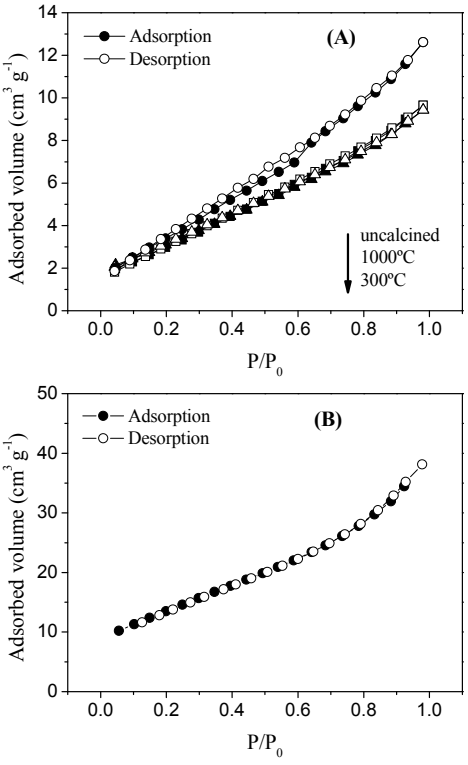

Figure 3. Adsorption-desorption isotherms of catalysts: (A) TiO_2 Kronos uncalcined and calcined at 300 and 1000ºC and (B) TiO_2 P25.

The results of specific surface area, total pores and micropores volume and mean pore diameter can be visualized in Table 1. The surface area of TiO_2 (Kronos) reduced after thermal treatment, while crystal size increased due to the sintering of small particles (Ferrari-Lima et al., 2013). The increase of the calcination temperature (from 300 to 1000ºC) caused no change in textural characteristics. TiO_2

Kronos had an area three-fold smaller than that of TiO_2 P25. The TiO_2-87 exhibited low porosity, while TiO_2 Kronos had no micropores, suggesting that the textural characteristics were determined during manufacture, independent of phase composition (rutile and anatase).

Table 1. Textural analysis results of TiO_2 samples.

Property	TiO_2 (Kronos)	TiO_2-100 (Kronos 300°C)	TiO_2-34 (Kronos 1000°C)	TiO_2-87 (P25)
Surface area ($m^2 g^{-1}$)	14.1	12.1	12.5	49.2
Total pores volume ($10^{-2} cm^3 g^{-1}$)	1.95	1.45	1.49	5.90
Micropores volume ($10^{-4} cm^3 g^{-1}$)	0.0	0.0	0.0	7.76
Mean pores diameter (Å)	55.3	48.4	47.9	47.9

The catalysts were analyzed by UV-Vis photoacoustic spectroscopy (PAS) and the graphs were constructed to obtain the bandgap energy, as shown in Figure 4a. The wavelength corresponding to the bandgap energy of the catalysts was determined from Equation 3.

$$\lambda = \frac{hC}{E_g} = \frac{1240}{E_g} \quad (3)$$

where:

λ is the wavelength (nm),

c is the speed of light in vacuum ($2.998x10^{17} nms^{-1}$),

h is Planck's constant (4.136×10^{-15} eVs) and

E_g is the bandgap energy (eV).

Table 2 shows the bandgap energies and wavelengths obtained using PAS analysis and pH_{ZPC} of catalysts. The catalysts have similar bandgap energies, with a slight reduction with the increase in the percentage of the rutile phase. The maximum photons absorption for TiO_2 was displaced to the visible region according to the increase in the proportion of rutile phase (after calcination), becoming an interesting condition for effluent treatment, which can be used alternative sources of irradiation, such as solar radiation.

Table 2. Bandgap energy, maximum photons absorption wavelength and pH_{ZPC} of the catalysts.

Catalyst	E_g (eV)	λ (nm)	pH_{ZPC}
TiO_2-34	3.0	413.3	6.9
TiO_2-87	3.1	400.0	6.1
TiO_2-100	3.2	387.5	6.3

In Figure 4b, it was obtained the emission spectrum of the germicide lamp used in the photodegradation reactions. Despite these lamps typically emit at 253.7 nm (UV-C), it was found emission peaks in the visible region of the electromagnetic spectrum, however only a small fraction from the visible light range is available to hydroxyl radicals generation. Emission peaks in the region around 365 and 400 nm matches the catalyst photo-excitation (λ < 413.3).

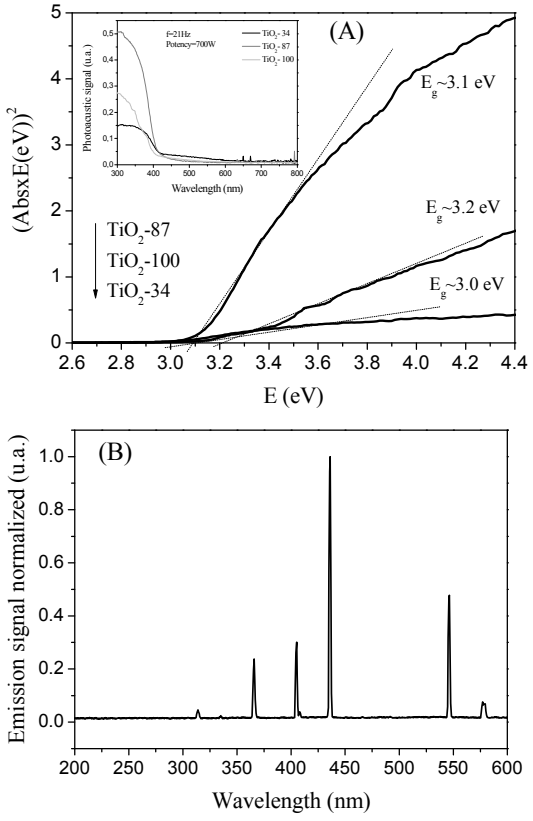

Figure 4. (A) Bandgap energy of catalysts. Inset: UV-Vis photoacoustic absorption spectra; (B) UV-Vis lamp emission spectrum.

The TiO_2 surface charges in liquid solution are driven by sample pH, allied with the zero point of charge (pH_{zpc}). The surface charge influences the substrate adsorption process and the amount of aggregates (Singh, Saquib, Haque, & Muneer, 2007), thus affecting photodegradation efficiency. The pH_{zpc} for TiO_2-87 was about 6.1 (Table 2) and the vinasse samples showed pH 4.7, which is below pH_{zpc}, indicating that the TiO_2 surface prevailed positively charged (predominance of Ti-OH_2^+ species). Therefore, this is a favorable condition (pH_{zpc} > pH) for that the adsorption process of vinasse on the catalyst surface occurs, due to electrostatic interactions, because in the vinasse mainly particles negatively charged or with high electron density/negative residual charges such as phenolic compounds (Chu & Wong, 2004) are present, favoring the photocatalytic process.

Vinasse characterization and pre-treatment

Table 3 exhibits the characterization results of the vinasse samples collected during the sugarcane crop/processing season (from November to January). The collected samples were non homogeneous and showed differences in color, turbidity and COD. These differences may also be attributable to the raw material used (molasses or sugarcane juice) to produce ethanol. It was found that the vinasse contains highly absorbing compounds and high turbidity values. The high COD suggests the presence of large amounts of organic pollutants in the vinasse.

Table 3. Results of the pH, COD, color and turbidity of the *in nature* vinasse samples*.

Sample	pH	COD (mg O_2 L^{-1})	Color (PtCo)	Turbidity (FTU)
1	4.78±0.27	55000±55	41000±39	4833±10
2	4.74±0.32	51540±51	24600±26	3095±7
3	4.65±0.29	58390±59	32600±30	3825±9
4	4.70±0.31	35150±49	31600±29	5800±12

*Results expressed as means values ± standard deviations of the triplicate.

The *in nature* vinasse samples were pre-treated by coagulation/flocculation process and the results are presented in Table 4. Despite several differences in the *in nature* vinasse samples (Table 3), the pre-treatment with Tanfloc®, a cationic polymer, led to similar percentage reduction of color, turbidity and COD in the samples (Table 4), without change of pH. Probably the high decrease in turbidity suggests that besides inorganic and organic compounds yeast was also dragged by the resulting sludge, which was of 350 mL per liter of vinasse. The high reduction of color and turbidity, higher than 80 and 90%, respectively, are indicative of coagulation/flocculation efficiency, however the COD values suggest the presence of high amount of organic compounds that remained in the effluent.

Table 4. Reduction of the color, turbidity and COD by coagulation/flocculation process*.

Sample	Color (455 nm)	Turbidity (860 nm)	COD (600 nm)
1	85%	97%	45%
2	84%	90%	40%
3	87%	93%	41%
4	80%	90%	45%

*Reduction percentage in terms of initial values (Table 3) in pH 4.7 (natural vinasse pH).

Photocatalytic degradation of vinasse

Three catalysts (TiO_2-100, TiO_2-34 and TiO_2-87) were evaluated in the photocatalytic degradation of vinasse (*in nature*, pre-treated and diluted). The photocatalytic efficiency was evaluated through the absorbance reduction at 270 nm (maximum absorption region of compounds in vinasse) and the results are illustrated in Figure 5. The kinetic profile indicates that the absorbance as a function of time obeys a linear relationship at the beginning of the reaction (up to 10 hours). The linearity indicates zero-order kinetic law. After 10 hours, the reaction behavior changes only for *in nature* vinasse samples (Figure 5a).

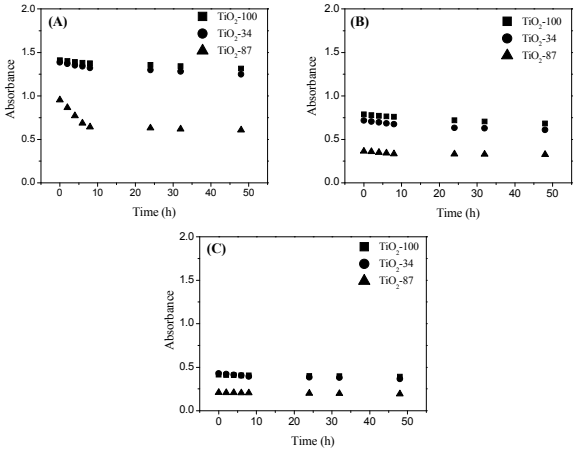

Figure 5. Photodegradation kinetics monitored at 270 nm: (A) *in nature*, (B) pre-treated and (C) diluted vinasse.

The kinetic behavior exhibited in Figure 5 can be rationalized by the Langmuir-Hinshelwood (L-H) mechanism. The L-H model is applied to photo-catalyzed heterogeneous systems once evolves an adsorption pre-equilibrium followed by a relatively slow reaction toward the products, which is represented by Equation 4 (Konstantinou & Albanis, 2004; Brites et al., 2011):

$$r = -\frac{dC}{dt} = \frac{kKC}{1 + KC} \quad (4)$$

where:

k is the rate constant,

K is the adsorption equilibrium constant and

C is the substrate concentration.

The values recorded in Table 4 indicate a high concentration of pollutants in the substrate, thus $K.C >> 1$. Equation 4 can be simplified, giving zero-order kinetic law (Equation 5 and 6):

$$r = -\frac{dC}{dt} = k \quad (5)$$

after integration, it becomes:

$$C - C_0 = -k.t \quad (6)$$

Taking into account the linear relationship between the substrate concentration and the absorbance (Abs), which is described by the Lambert-Beer law, the resulting expression is (given

by Equation 7; therefore, the obtained constants rate were taken from the initial photoreaction region (up to 10 hours) in all cases.

$$Abs = Abs_o - k.t \quad (7)$$

Organic matter adsorption is necessary for photocatalysis. However, as expected, the amount of materials adsorbed cannot be very large in the presence of a large excess of organic pollutants, which block light to the catalyst active sites, and due to light scattering produced by the suspended materials. Both effects diminish the photocatalytic efficiency (Gogate & Pandit, 2004). Thus, the formation of electron-hole pair from the activation of catalyst is important, because the positive hole can act as an oxidizing agent from the adsorption of pollutant molecules, causing the oxidation process. In addition, H_2O or OH^- molecules present in the medium can be adsorbed into the positive holes and generate the hydroxyl radicals to oxidize the pollutant. Furthermore, the presence of electron in the conduction band can react to form another radicals species, such as peroxyl ($O_2^{\bullet-}$) and hydroperoxyl ($HO_2^{\bullet}$) capable of oxidizing the substrate and form intermediates which by means of subsequent oxidations reach the mineralization. The hydroxyl radical is considered the main oxidant species during TiO_2 photo-excitation.

The results of kinetics fit to *in nature*, pre-treated and diluted vinasse can be observed in Table 5. The COD reduction of the vinasse samples after photolysis (without catalyst) is included for comparison. The COD results show that the photocatalysis efficiency was much higher than the photolysis. In a previous work, Santana and Fernandes-Machado (2008) reported that the photolysis is inefficient in the mineralization of vinasse, indicating the importance of photocatalysts in vinasse treatment. TiO_2-100 and TiO_2-87 had similar efficiency in COD reduction as *in nature* vinasse; however, they were less efficient than TiO_2-34. Although TiO_2-87 had a higher degradation rate (k, monitored for 10 hours), TiO_2-34 was the most efficient in COD removal. The low COD reduction after photodegradation found in all experiments may lead to wrong interpretations. It was a consequence of the high initial turbidity of *in nature* vinasse which made light penetration difficult.

The photodegradation of pre-treated vinasse improved the quality of effluent, as demonstrated by the data in Table 5. The catalyst containing 100% anatase phase had the lowest efficiency, reinforcing that a mixture of anatase and rutile may be important to increase the catalytic activity. In fact, as also observed by other authors (Bacsa & Kiwi, 1998), the results indicate that the catalysts containing only either anatase or rutile are less efficient than those containing both phases. TiO_2-87 and TiO_2-34 showed similar rate constants. However, TiO_2-87 presented the highest COD reduction, which made it the best photocatalyst. Such efficiency can be attributed to the lower rutile phase content of the catalyst (Ding, Lu, & Greenfield, 2000; Saadoun et al., 1999) because the reduction of the rutile content is related to the increase of the number of water and hydroxyl groups adsorbed onto the surface, which are crucial for photocatalytic reaction (Saadoun et al., 1999). These results indicate that the use of a catalyst with more than 13% of rutile may be promising for the photocatalytic treatment of vinasse, as it may replace TiO_2 P25 (TiO_2-87), including in the treatment of other types of industrial effluents.

Table 5. Results of kinetics fit to *in nature*, pre-treated and diluted vinasse after photocatalysis.

Catalyst	*in nature*			pre-treated Tanfloc®			diluted 1:2 (v v^{-1})		
	k (h^{-1})	R^2	% Red COD	k (h^{-1})	R^2	% Red COD	k (h^{-1})	R^2	% Red COD
Photolysis	-	-	1.7	-	-	3.4	-	-	7.2
TiO_2-100	0.0045	0.9912	5.2	0.0037	0.9848	5.8	0.0012	0.9889	11.0
TiO_2-34	0.0080	0.9966	8.3	0.0040	1.0000	16.4	0.0044	0.9944	16.8
TiO_2-87	0.0400	0.9871	5.4	0.0041	0.9959	22.8	0.0007	0.9868	10.3

To diluted (1:2, v v^{-1}) vinasse samples (Table 5), the photolysis showed low COD reduction and photocatalysis was more efficient. The best results were obtained with the catalyst with the lowest anatase content (TiO_2-34), while the efficiency of TiO_2-87 was different from that obtained with pre-treated samples. For TiO_2-34, the rate constant and COD reduction results were similar to those obtained with pre-treated vinasse. However, dilution has the disadvantage that increases the volume of vinasse, which is already large. The dilution and coagulation/flocculation processes provided a greater light penetration due to the decrease in the amount of interferents that compete for photons and/or produce light scattering. Wastewater treatment previous to photocatalysis is necessary.

Figure 6 presents results of the reduction of absorbance after photo reaction during 48 hours at 270 nm (maximum absorption wavelength, 254 nm (aliphatic region), 284 nm (aromatic groups), 310 nm (conjugated aromatic rings) and 500 nm (visible light-absorbing chromophores). In Figure 6a, it can be observed that TiO_2-87 catalyst

has high photoactivity in the reduction of absorbance at all the wavelengths analyzed, despite the low COD reduction. Results suggest the formation of intermediate reaction compounds not completely mineralized. Among the catalysts, both TiO_2-34 and TiO_2-87 promoted absorbance reduction in the visible region, 500 nm. In terms of absorbance reduction of pre-treated vinasse (Figure 6b), the behavior of all catalysts was very similar with TiO_2-87 being less efficient at all measured wavelengths. Through Figure 6c, it was found that once again TiO_2-34 showed the best photoactivity; even at 500 nm exhibited the highest absorbance reduction.

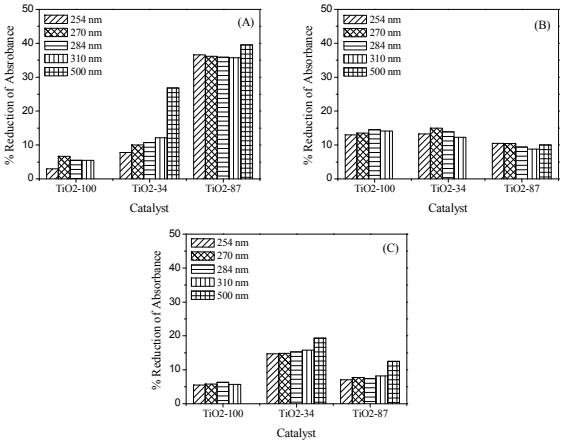

Figure 6. Reduction of absorbance intensity for: (A) *in nature*, (B) pre-treated and (C) diluted vinasse samples after 48 hours photodegradation monitored at several wavelengths.

Bioassays for toxicity evaluation: *Artemia salina*

For the determination of Lethal Concentration (LC_{50}), it was evaluated the concentration of vinasse (mg L^{-1}) responsible for 50% mortality of *Artemia salina*, with results estimated by the Reed-Muench plot. The toxicity of the sample is inversely proportional to the LC_{50} (more toxic to the lower LC_{50}). A potassium dichromate solution was taken as reference and it exhibited a LC_{50} of 16 mg L^{-1}. Table 6 gives the lethal concentrations (LC_{50}) and the toxicity reduction of vinasse samples after photocatalytic treatment based on toxicity of *in nature* vinasse. In all experiments, treated vinasse was less toxic indicating the partial mineralization or separation of the toxic organic matter in the samples. The results after photodegradation agree with the COD reduction results (Table 5) with a few variations.

In all experiments, TiO_2-87 catalyst gave the lethal concentration, indicating the lower toxicity of the samples after treatment. The performance of TiO_2-87 was closely followed by that of TiO_2-34, which was only ~6% lower. The results in Table 6 demonstrate that the catalyst with 100% anatase is not as efficient as the catalyst with mixed anatase-rutile phase. Such behavior can also be related to the bandgap energy of these catalysts. Also again, photolysis was not efficient. *In nature* vinasse had a LC_{50} of 8.7 mg L^{-1} but its toxicity was reduced significantly after photocatalysis, while the toxicity of pre-treated and diluted vinasse diminished by ≈10 times after treatment with TiO_2-87. Despite this good result, the pre-dilution increased the amount of effluent. Thus, the best pre-treatment in terms of COD and toxicity was the coagulation/flocculation process.

Table 6. Lethal concentration (LC_{50}) and toxicity reduction of vinasse samples based on *in nature* vinasse toxicity.

Catalyst	*in nature*		pre-treated Tanfloc®		diluted 1:2 (v v^{-1})	
	LC_{50} (mg L^{-1})	Toxicity reduction*	LC_{50} (mg L^{-1})	Toxicity reduction*	LC_{50} (mg L^{-1})	Toxicity reduction*
Photolysis	19.0	1.2	22.0	1.5	48.0	4.5
TiO_2-100	35.0	3.0	50.0	4.8	54.0	5.2
TiO_2-34	48.0	4.5	63.0	6.2	74.0	7.5
TiO_2-87	51.0	4.9	85.0	8.8	85.0	8.8

*The LC_{50} reference value of *in nature* vinasse is 8.7 mg L^{-1}.

Conclusion

The results showed that despite the slight COD decrease of *in nature* vinasse, its toxicity was significantly reduced after photocatalytic treatment, especially when TiO_2-34 and TiO_2-87 were used. This behavior shows that the mixture of anatase and rutile phases showed a positive synergistic effect. Regarding pre-treatment of vinasse, the coagulation/flocculation process was more efficient, promoting the greatest reductions of COD (67%) and toxicity (up to 10 times). although the photocatalytic treatment of the diluted vinasse has been effective, this combination is not beneficial because of the large increase in the sample volume to be treated becoming it an unfeasible method. Therefore, photocatalysis combined to the coagulation/flocculation was effective on the vinasse degradation.

Acknowledgements

The authors would like to acknowledge Professor Noboru Hioka, for your significant contribution in elaboration of this work and the Brazilian agencies CNPq, Capes and Fundação Araucária for the financial support.

References

Ahmed, S., Rasul, M. G., Brown, R., & Hashib, M. A. (2011). Influence of parameters on the heterogeneous

photocatalytic degradation of pesticides and phenolic contaminants in wastewater: A short review. *Journal of Environmental Management, 92*(3), 311-330.

American Public Health Association (APHA). (1999). *Standard methods for the examination for water and wastewater* (20th ed.). Washington, DC: Pharmabooks.

Andreozzi, R., Caprio, V., Insola, A., & Marotta, R. (1999). Advanced oxidation processes (AOP) for water purification and recovery. *Catalysis Today*, *53*(1), 51-59.

Bacsa, R. R., & Kiwi, J. (1998). Effect of rutile phase on the photocatalytic properties of nanocrystalline titania during the degradation of p-coumaric acid. *Applied Catalysis B: Environmental, 16*(1), 19-29.

Boroski, M., Rodrigues, A. C., Garcia, J. C., Sampaio, L. C., Nozaki, J., & Hioka, N. (2008). The effect of operational parameters on electrocoagulation–flotation process followed by photocatalysis applied to the decontamination of water effluents from cellulose and paper factories. *Journal of Hazardous Materials, 160*(1), 135-141.

Brites, F. F., Santana, V. S., & Fernandes-Machado, N. R. C. (2011). Effect of support on the photocatalytic degradation of textile effluents using Nb_2O_5 and ZnO: Photocatalytic degradation of textile dye. *Topic in Catalysis, 54*(1), 264-269.

Chu, W., & Wong, C. C. (2004). The photocatalytic degradation of dicamba in TiO_2 suspensions with the help of hydrogen peroxide by different near UV irradiations. *Water Research, 38*(4), 1037-1043.

Cibis, E., Ryznar-Luty, A., Krzywonos, M., & Miskiewicz, T. (2007). Aerobic biodegradation of vinasse: Effect of temperature, initial pH and pH control. *Journal of Biotechnology, 131S*(2), S155-S156.

Couto Junior, O. M., Barros, M. A. S. D., & Pereira, N. C. (2013). Study on coagulation and flocculation for treating effluents of textile industry. *Acta Scientiarum. Technology, 35*(1), 83-88.

Ding, Z., Lu, G. Q., & Greenfield, P. F. (2000). Role of the crystallite phase of TiO_2 in heterogeneous photocatalysis for phenol oxidation in water. *Journal of Physical Chemistry B, 104*(19), 4815-4820.

Fernandes-Machado, N. R. C., & Santana, V. S. (2005). Influence of thermal treatment on the structure and phocatalytic activity of TiO_2 P-25. *Catalysis Today, 107*(30), 595-601.

Ferrari-Lima, A. M., Marques, R. G., Fernandes-Machado, N. R. C., & Gimenes, M. L. (2013). Photodegradation of petrol station wastewater after coagulation/flocculation with tannin-based coagulant. *Catalysis Today, 209*, 79-83.

Furtado, A. T., Scandiffio, M. I. G., & Cortez, L. A. B. (2011). The Brazilian sugarcane innovation system. *Energy Policy, 39*(1), 156-166.

Garcia, J. C., Simionato, J. A., Silva, A. E. C., Nozaki, J., & Souza, N. E. (2009). Solar photocatalytic degradation of real textile effluents by associated titanium dioxide and hydrogen peroxide. *Solar Energy, 83*(3), 316-322.

Gogate, P. R., & Pandit, A. B. (2004). A review of imperative technologies for wastewater treatment I: oxidation technologies at ambient conditions. *Advances in Environmental Research, 8*(3-4), 501-551.

Joint Committee on Powder Diffraction Standars (1995). *International center of diffraction data* [CDROM]. Newtown Square, PA: 19073.

Konstantinou, I. K., & Albanis, T. A. (2004). TiO_2-assisted photocatalytic degradation of azo dyes in aqueous solution: kinetic and mechanistic investigations: A review. *Applied Catalysis B: Environmental, 49*(1), 1-14.

Linsebigler, A. L., Lu, G., & Yates, J. T. JR. (1995). Photocatalysis on TiO_2 surfaces: Principles, mechanisms and selected results. *Chemical Reviews, 95*(3), 735-758.

Martín, M. A., Raposo, F., Borja, R., & Martn, A. (2002). Kinetic study of anaerobic digestion of vinasse pretreated with ozone, ozone plus ultraviolet light and ozone plus ultraviolet light in the presence of titanium dioxide. *Process Biochemistry, 37*(7), 699-706.

Mohana, S., Acharya, B. K., & Madamwar, D. (2009). Distillery spent wash: treatment technologies and potential applications. *Journal of Hazardous Materials, 163*(1), 12-25.

Nogueira, R. F. P., & Jardim, W. F. (1998). A fotocatálise heterogênea e sua aplicação ambiental. *Química Nova, 21*(1), 69-72.

Robert, D., & Malato, S. (2002). Solar photocatalysis: a clean process for water detoxification. *The Science of the Total Environment, 291*(1-3), 85-97.

Rosabal, A., Morillo, E., Undabeytia, T., Maqueda, C., Justo, A., & Herencia, J. F. (2007). Long-term impacts of wastewater irrigation on Cuban soils. *Soil Science Society of America Journal, 71*(4), 1292-1298.

Saadoun, L., Ayllón, J. A., Jiménez-Becerril, J., Peral, J., Doménech, X., & Rodríguez-Clemente, R. (1999). 1-2-Diolates of Titanium as suitable precursors for the preparation of photoactive high surface titania. *Applied Catalysis B: Environmental, 21*(4), 269-277.

Santana, V. S., & Fernandes-Machado, N. R. C. (2008). Photocatalytic degradation of the vinasse under solar radiation. *Catalysis Today, 133-135*, 606-610.

Santana, V. S., Alberton, A. L., & Fernandes-Machado, N. R. C. (2005). Influence of luminous intensity on textile effluent photodegradation. *Acta Scientiarum. Technology, 27*(1), 1-6.

Sharma, S., Sharma, A., Singh, P. K., Soni, P., Sharma, S., Sharma, P., & Sharma, K. P. (2007). Impact of distillery soil leachate on haematology of Swiss albino mice (Mus musculus). *Bulletin of Environmental Contamination and Toxicology, 79*(3), 273-277.

Silva, M. A. S., Griebeler, N. P., & Borges, L. C. (2007). Uso de vinhaça e impactos nas propriedades do solo e lençol freático. *Revista Brasileira de Engenharia Agrícola e Ambiental, 11*(1), 108-114.

Singh, H. K., Saquib, M., Haque, M. M., & Muneer, M. (2007). Heterogeneous photocatalysed degradation of 4-chlorophenoxyacetic acid in aqueous suspensions. *Journal of Hazardous Materials, 142*(1-2), 374-380.

Souza, R. P., Girardi, F., Santana, V. S., Fernandes-Machado, N. R. C., & Gimenes, M. L. (2013). Vinasse treatment using a vegetable-tannin coagulant and photocatalysis. *Acta Scientiarum. Technology, 35*(1), 89-95.

União da Indústria de Cana-de-Açúcar (Unica). (2015). *Setor Sucroenergético*. São Paulo, SP: Cdn Comunicação. Recuperado de http://www.unica.com.br

Yang, J., Li, D., Wang, X., Yang, X., & Lu, L. (2002). Synthesis and microstructural control of nanocrystalline titania powders via a stearic acid method. *Materials Science and Engineering, A328*(1-2), 108-112.

Received on April 16, 2014.
Accepted on September 1, 2015.